

Time dependent dispersion of nanoparticles in blood vessels

Francesco Gentile¹, Paolo Decuzzi²

¹Center of Bio-Nanotechnology and -Engineering for Medicine, Università Magna Graecia, Catanzaro, Italy;

²Department of Nanomedicine and Biomedical Engineering, the University of Texas Health Science Center, Houston, USA.

Email: gentile@unicz.it

Received 25 September 2009; revised 20 October 2009; accepted 25 October 2009.

ABSTRACT

The dispersion of intravascularly injected nanoparticles can be efficiently described by introducing an effective diffusion coefficient D_{eff} which quantifies the longitudinal mass transport in blood vessels. Here, the original work of Gill and Sankarasubramanian was modified and extended to include 1) the variation over time of D_{eff} ; 2) the permeability of the blood vessels and 3) non-Newtonian rheology of blood. A general solution was provided for D_{eff} depending on space (ζ), time (τ), plug radius (ξ_c) and a subset of permeability parameters. It was shown that increasing the vessel plug radius (thus hematocrit) or permeability leads to a reduction in D_{eff} , limiting the transport of nanoparticles across those vessels. It was also shown that the asymptotic time beyond which the solution attains the steady state behaviour is always independent of the plug radius and wall permeability. The analysis presented can more accurately predict the transport of nanoparticles in blood vessels, compared to previously developed models.

Keywords: Nanoparticle Transport; Casson Fluid; Permeable Blood Vessels; Drug Delivery

1. INTRODUCTION

The study of solute dispersion in capillaries dates back to the celebrated works of Taylor and Aris [1,2], who first studied the effect of shear stress on the transport in laminar flows. They provided a solution for the classic advection/diffusion equation

$$\frac{\partial C}{\partial t} + \mathbf{u} \cdot \nabla C = D_m \nabla^2 C \quad (1)$$

in the long term steady state limit, in terms of a constant effective coefficient of diffusion as

$$D_{eff} = D_m \left(1 + \frac{P_e^2}{192} \right), \quad (2)$$

which includes the molecular diffusion contribution (\propto

D_m) and the convective contribution ($\propto P_e$). In the Eqs. 1 and 2 above, P_e ($P_e = R_e \times u_0 / D_m$) is the Peclet number for a capillary with radius R_e and centerline velocity u_0 , C is the local solute concentration; \mathbf{u} is the fluid velocity vector; D_m is the Brownian or molecular diffusion coefficient and ∇ and ∇^2 are the gradient and Laplacian operators, respectively. The solution of Taylor and Aris is valid under the simplifying assumptions of 1) quasi-steady dispersion and 2) unidirectional flow. In particular, it is strictly valid beyond the asymptotic time $t_{st} = 1/2 \times R_e^2 / D_m$. Notice that sub-micrometric particles with a molecular diffusivity D_m typically ranging between 10^{-11} and 10^{-9} m²/s, in large vessels ($R_e \cong 10^{-2}$ m) would have t_{st} of the order of 10^5 - 10^7 s, whereas in small capillaries ($R_e \cong 10^{-6}$ m) t_{st} would fall in the range 10^{-3} - 10^{-1} s.

Considerable efforts were expended in the attempt of relaxing the above assumptions. Gill [3] extended Taylor's formulation to obtain the local concentration C by means of a series expansion about the mean concentration, leading to the Generalized Dispersion Model (GDM), founding upon the rephrased convective-diffusive equation

$$\frac{\partial \Psi_m}{\partial \tau} = \sum_{i=0}^{\infty} K_i(t) \frac{\partial^i \Psi_m}{\partial \zeta^i} \quad (3)$$

where $K_i(t)$ are suitable functions of time; Ψ_m is the normalized concentration averaged over a cross section of the capillary as explained in the sequel, ζ and τ are the longitudinal and time coordinates respectively. Sankarasubramanian and Gill [4] further developed the GDM including the effect of wall permeability to the solute (*i.e.* nanoparticles). In 1993, Sharp derived explicit expressions for the constant steady state coefficient D_{eff} for a non-Newtonian fluid considering, in particular, a Casson-like fluid [5]. Dash *et al.* [6] and Nagarani *et al.* [7] combined the model of Sharp and the GDM to obtain the unsteady dispersion in a Casson-like fluid, introducing solute adsorption to the walls. More recently, Decuzzi *et al.* [8] revisited the theory of Taylor and Aris incorporating the effects of wall permeability for the working fluid (plasma) and deriving a novel and more general

expression for D_{eff} being

$$D_{eff} = D_m \left[1 + \frac{P_{e_0}^2}{192} \times f(\Omega, \Pi, \tilde{z}) \right] \quad (4)$$

where P_{e_0} is the Peclet number at the entrance of the capillary ($\tilde{z} = 0$), and f is a function of the permeability parameter Π , pressure parameters Ω , and longitudinal coordinate \tilde{z} along the capillary, as described in the sequel. In 2008, Gentile *et al.* [9] expanded the solution in [8] to include a Casson-like model for the fluid. Noticeably, the models presented in [8] and [9] are valid in the limit of large times of dispersion or, equivalently, at the steady state. No explicit dependency on time was introduced and the solution was deduced in terms of the longitudinal space coordinate solely.

In this work, the transport formulation proposed in [9] was further developed to account for the time dependency of the problem. The transport of nanoparticles was investigated and the effective diffusion coefficient D_{eff} derived. D_{eff} would in general depend upon the permeability of the capillary and the rheology of blood as in [9], but this dependency was extended to all times, thus also comprising the initial regime of dispersion. The model presented herein comprises, in the limits, well established schemes of diffusion.

2. MATERIALS AND METHODS

A circular capillary with radius Re and length l was considered as in **Figure 1**. A Casson-like fluid was considered with capillary walls permeable to the fluid, impermeable and not adsorbent to the solute (*i.e.* nanoparticles). In the following of the paper, the Generalized Dispersion Model was recalled and revised.

2.1. The Governing Equations

Following [4], the dispersion of a solute in a cylindrical capillary was described by the normalized advection-diffusion equation

$$\frac{\partial \Psi}{\partial \tau} + v \frac{\partial \Psi}{\partial \zeta} = \left(\frac{1}{\rho} \frac{\partial}{\partial \rho} \left(\rho \frac{\partial}{\partial \rho} \right) + \frac{1}{P_{e_0}^2} \frac{\partial^2}{\partial \zeta^2} \right) \Psi \quad (5)$$

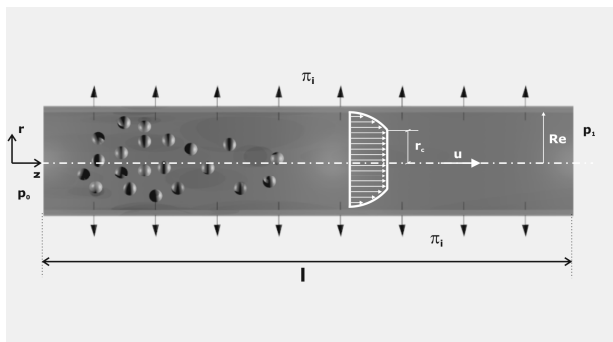


Figure 1. Longitudinal transport of molecules or nanoparticles in a blood capillary with a blunted velocity profile.

with the non dimensional terms being

$$\begin{aligned} \Psi &= \frac{C}{C_0}; \quad v = \frac{u}{u_0}; \quad \rho = \frac{r}{R_e}; \\ \zeta &= \frac{D_m z}{R_e^2 u_0}; \quad \tau = \frac{D_m t}{R_e^2}; \end{aligned} \quad (6)$$

where C is the local concentration of the solute and C_0 a reference concentration, u_0 is the initial center line velocity at the inlet and u the velocity distribution within the capillary with radius R_e , D_m is the molecular diffusivity of the solute, r and z are the radial and longitudinal coordinates as from the frame of reference in **Figure 1**, and t stays for the dimensional time. In **Eq.6** P_{e_0} ($= R_e \times u_0/D_m$) is the characteristic Peclet number defined as above. It was assumed that the particles are sufficiently small to have the same velocity of the dislodging fluid so that the diffusion/advection problem and the fluid-dynamic problem may be treated separately. The solution of **Eq.5** for Ψ can be derived *exactly* as

$$\Psi = \sum_{i=0}^{\infty} f_i(\rho, \zeta; \tau) \frac{\partial^i \Psi_m}{\partial \zeta^i} \quad (7)$$

where the functions f_i were related to the i -th derivative of Ψ_m as shown in the sequel. The mean concentration Ψ_m was defined as

$$\Psi_m = 2 \int_0^1 \Psi \rho d\rho. \quad (8)$$

From **Eqs.5** and **7**, it follows that Ψ_m has to satisfy the relation

$$\frac{\partial \Psi_m}{\partial \tau} = \sum_{i=0}^{\infty} K_i \frac{\partial^i \Psi_m}{\partial \zeta^i} \quad (9)$$

where the dispersion coefficients K_i were defined properly as function of time as to give

$$\begin{aligned} K_i(\zeta, \tau) &= \frac{\delta_{i2}}{P_{e_0}^2} + 2 \frac{\partial f_i}{\partial \rho}(1, \zeta; \tau) - \\ &= -2 \int_0^1 f_{i-1}(\rho, \zeta; \tau) v(\rho, \zeta) \rho d\rho \end{aligned} \quad (10)$$

with the understanding that $f_0 = 1$ and $f_1 = 0$. Here δ_{i2} denotes the delta of Kronecker. The dispersion problem was thus reduced to estimating f_i and K_i for each i . The auxiliary functions f_i must satisfy the differential equations

$$\frac{\partial f_n}{\partial \tau} = \frac{1}{\rho} \frac{\partial}{\partial \rho} \left(\rho \frac{\partial f_n}{\partial \rho} \right) - v f_{n-1} + \frac{f_{n-2}}{P_{e_0}^2} - \sum_{i=0}^{\infty} K_i f_{n-i}. \quad (11)$$

Relations **Eq.10** and **Eq.11** are coupled, and their solution becomes untractable of $i > 2$. Nevertheless it was shown [10] that all terms involving a coefficient higher than $i = 2$ in **Eq.10** can be neglected, in that K_2 is more than two orders of magnitude greater than K_3 . **Eq.9** thus

reduces to the simplified relation

$$\frac{\partial \Psi_m}{\partial \tau} = K_1 \frac{\partial \Psi_m}{\partial \zeta} + K_2 \frac{\partial^2 \Psi_m}{\partial \zeta^2} \tag{12}$$

where K_1 and K_2 represent the convective and diffusive term, respectively. Notice that K_i and f_i depend upon the velocity field in the capillary $v(\rho, \zeta)$.

2.2. The Velocity Distribution in Permeable Capillaries

The velocity distribution in the capillary was given for a Casson-like fluid by [9]

$$v = -\frac{d\chi}{d\zeta} \times \begin{cases} 1 - \frac{8}{3}\xi_c^{1/2} + 2\xi_c - \frac{1}{3}\xi_c^2 & \text{for } \rho < \xi_c \\ -1 + \rho^2 + \frac{8}{3}(1 - \rho^{3/2})\xi_c^{1/2} - 2(1 - \rho)\xi_c & \text{for } \rho > \xi_c \end{cases} \tag{13}$$

where ξ_c is the ratio between the plug radius r_c and the radius of the capillary R_c ($\xi_c = r_c/R_c$) and $d\chi/d\zeta$ is the pressure gradient along ζ . From **Eq.13** the non dimensional flow rate was derived through integration over the cross section to give

$$\Theta = 2\pi \int_0^1 v(\rho) \rho d\rho = -\frac{\pi}{2} \frac{d\chi}{d\zeta} A(\xi_c), \tag{14}$$

where

$$A(\xi_c) = 1 - \frac{16}{7}\sqrt{\xi_c} + \frac{4}{3}\xi_c - \frac{1}{21}\xi_c^4, \tag{15}$$

and the mean fluid velocity could be written as

$$\Upsilon = \frac{\Theta}{\pi} = -\frac{1}{2} \frac{d\chi}{d\zeta} A(\xi_c). \tag{16}$$

In the limit of a Newtonian fluid ($\xi_c \rightarrow 0$), **Eq.16** yields the expected value $\Upsilon = 0.5$.

In permeable capillaries, the fluid flows laterally across the walls inducing a continuous reduction in mean fluid velocity along the capillary. Following [8,9], the normalized mean fluid velocity Υ was expressed as a function of the hydraulic conductivity L_p , the interstitial fluid pressure π_i , the inlet and the outlet vascular pressures p_0 and p_1 , giving

$$\Upsilon = -\frac{1}{2} \frac{d\chi}{d\zeta} A(\xi_c) = \frac{\cosh(\kappa\zeta\Gamma(\xi_c)) - \Omega \cosh(\Gamma(\xi_c) - \kappa\zeta\Gamma(\xi_c))}{1 - \Omega \cosh(\Gamma(\xi_c))} \frac{A(\xi_c)}{2}, \tag{17}$$

where Ω is a non dimensional pressure parameter

$$\Omega = \frac{p_0 / \pi_i - 1}{p_1 / \pi_i - 1}, \tag{18}$$

$\Gamma(\xi_c)$ is the permeability parameter given by

$$\Gamma(\xi_c) = \frac{4l}{R_e} \sqrt{\frac{\eta}{R_e}} L_p \frac{1}{\sqrt{A(\xi_c)}} = \frac{\Pi}{\sqrt{A(\xi_c)}}. \tag{19}$$

Notice that differently from [8], the permeability parameter Γ is not fixed and varies with ξ_c . Substituting back the **Eqs.17** and **13** to **Eqs.10** and **11**, the coefficients K_i were appropriately derived.

2.3. The Initial and Boundary Conditions

It was assumed that a bolus of nanoparticles is introduced instantaneously and uniformly at the initial time $t = 0$ into the capillary, that is

$$\Psi(\rho, \zeta; 0) = \Psi_m(\zeta; 0). \tag{20}$$

In addition, the walls are impermeable to the solute and no absorption occurs to lead to

$$\left. \frac{\partial \Psi}{\partial \rho} \right|_{\rho=1} = 0, \tag{21}$$

symmetry at the centerline imposed

$$\left. \frac{\partial \Psi}{\partial \rho} \right|_{\rho=0} = 0, \tag{22}$$

and finally mass conservation was translated in mathematical terms as

$$\Psi|_{\zeta \rightarrow \infty} = \frac{\partial^i \Psi}{\partial \zeta^i} \Big|_{\zeta \rightarrow \infty} = 0; \quad \Psi_m|_{\zeta \rightarrow \infty} = \frac{\partial^i \Psi_m}{\partial \zeta^i} \Big|_{\zeta \rightarrow \infty} = 0; \quad i > 0. \tag{23}$$

The above relations should be also rephrased in terms of f_i to solve **Eq.11**, giving [4,6,7]

$$\int_0^1 f_i \rho d\rho = \delta_{0i}, \quad \left. \frac{\partial f}{\partial \rho} \right|_{\rho=1} = 0, \quad \left. \frac{\partial f}{\partial \rho} \right|_{\rho=0} = 0. \tag{24}$$

2.4. Solution for K_1 and f_1

Imposing $n = 1$ in **Eq.11**, it was derived

$$\frac{\partial f_1}{\partial \tau} = \frac{1}{\rho} \frac{\partial}{\partial \rho} \left(\rho \frac{\partial f_1}{\partial \rho} \right) - v - K_1, \tag{25}$$

and multiplying by ρ and integrating with respect to ρ from 0 to 1, invoking the first of **Eq.24**, it followed that

$$K_1 = -2 \int_0^1 v \rho d\rho = -\Upsilon(\zeta). \tag{26}$$

From **Eq.26**, it was deduced that the convective term K_1 equals the mean velocity Υ that is not constant along the capillary. Also notice that assuming a frame of reference moving with Υ , K_1 would be zero as in [6]. f_1 was found as a solution of the partial differential **Eq.25**

that can be decomposed as the sum the steady state solution $f_{1s}(\rho, \zeta)$ and the transient term $f_{1t}(\rho, \zeta; \tau)$.

$$f_1(\rho, \zeta; \tau) = f_{1s}(\rho, \zeta) + f_{1t}(\rho, \zeta; \tau). \tag{27}$$

Substitution of the steady state term f_{1s} into **Eq.25** yield

$$\frac{1}{\rho} \frac{\partial}{\partial \rho} \left(\rho \frac{\partial f_{1s}}{\partial \rho} \right) = \nu - \Upsilon; \tag{28}$$

which holds in the core of the capillary ($\rho < \xi_c$), where the velocity is blunted, and in the cell free layer ($\rho > \xi_c$), where the velocity varies with ρ . At the interface, $\rho = \xi_c$, continuity imposed that $f_{1s}(\rho = \xi_c^-) = f_{1s}(\rho = \xi_c^+)$ which, together with the boundary conditions **Eq.24**, allowed the deconvolution of f_{1s} as

$$f_{1s}(\rho, \zeta) = \frac{\cosh(\kappa \zeta \Gamma(\xi_c)) - \Omega \times \cosh(\Gamma(\xi_c) - \kappa \zeta \Gamma(\xi_c))}{1 - \Omega \cosh(\Gamma(\xi_c))} \times \begin{cases} B(\rho) & \text{for } \rho < \xi_c \\ C(\rho) & \text{for } \rho > \xi_c \end{cases} \tag{29}$$

where B and C are solely functions of ρ :

$$B(\rho; \xi_c) = \frac{-8085 + 21600 \xi_c^{1/2} - 15092 \xi_c + 1430 \xi_c^4}{194040} + \frac{147 \xi_c^6 + 1155(21 - 64 \xi_c^{1/2} + 56 \xi_c - 14 \xi_c^2 + \xi_c^4) \rho^2}{194040} - \frac{2310 \xi_c^4 \ln(\xi_c)}{194040}, \tag{30}$$

$$C(\rho; \xi_c) = -\frac{1}{48} (2 - 6\rho^2 + 3\rho^4) + \frac{4}{1617} (45 - 154\rho^2 + 88\rho^{7/2}) \xi_c^{1/2} - (7 + 10\rho^2(2\rho - 3)) \xi + \frac{(2\rho^2 - 3)}{336} \xi^4 + \frac{\xi^6}{1320} - \frac{\xi^4}{84} \ln(r). \tag{31}$$

The transient term f_{1t} depends upon f_{1s} and was readily derived as [6]

$$\sum_{n=0}^{\infty} \frac{J_0(\lambda_n \rho) f_{1s}(\rho, \zeta) \rho d\rho}{J_0(\lambda_n)^2} e^{-\lambda_n^2 \tau} J_0(\lambda_n \rho) \tag{32}$$

where J_0 and J_1 are the Bessel function of first type and order zero and one, respectively, and the eigenvalues λ_n were found as the roots of the equation $J_1(\lambda_n) = 0$.

2.5. Solution for K_2

Imposing $n = 2$ in **Eq.11**, multiplying by ρ and integrat-

ing with respect to ρ from 0 to 1, K_2 was obtained as

$$K_2(\zeta; \tau) = \frac{1}{Pe_0^2} - 2 \int_0^1 f_1(\rho, \zeta; \tau) \nu(\rho, \zeta) \rho d\rho \tag{33}$$

notice that, differently from the original formulation by Gill and Sankarasubramanian [4,10], the auxiliary functions K_2 would in general depend also on the longitudinal coordinate ζ and, in particular, the problem would be determined if the velocity field in the capillary is known. In the limit of large time K_2 is found as

$$K_2(\zeta) \Big|_{\tau \rightarrow \infty} = \frac{1}{Pe_0^2} + \frac{1}{192} \frac{\cosh(\kappa \zeta \Gamma(\xi_c)) - \Omega \times \cosh(\Gamma(\xi_c) - \kappa \zeta \Gamma(\xi_c))}{1 - \Omega \cosh(\Gamma(\xi_c))} \times \left(1 - \frac{5888}{1555} \xi_c^{1/2} + \frac{558368}{56595} \xi_c - \frac{6144}{715} \xi_c^{3/2} + \frac{128}{45} \xi_c^2 + \frac{244}{21} \xi_c^4 - \frac{272128}{3773} \xi_c^{9/2} + \frac{385312}{2205} \xi_c^5 - \frac{4096}{21} \xi_c^{11/2} + \frac{11464}{165} \xi_c^6 + \frac{55808}{1155} \xi_c^{13/2} - \frac{6976}{165} \xi_c^7 + \frac{430331}{66885} \xi_c^8 - \frac{512}{147} \xi_c^{17/2} + \frac{64}{21} \xi_c^9 - \frac{872}{1155} \xi_c^{10} + \frac{4}{147} \xi_c^{12} - \frac{8}{147} \xi_c^8 \ln(\xi_c) \right) \tag{34}$$

thus recovering the results derived in [9]. Incidentally notice that **Eq.34** represents the most general formulation for the non dimensional coefficient of diffusion K_2 in that it comprises an extensive subset of solutions, depending on the rheological parameters ξ_c , Γ and Ω . In particular, as Γ (or, equivalently, Π) goes to zero (impermeable capillary) **Eq.34** coincides with the relation given in [5], whereas as the rheological parameter ξ_c goes to zero the result given by [8] is recovered. The classical solution of Taylor and Aris [1,2] is found when both $\Gamma(\Pi)$ and ξ_c are null.

3. RESULTS AND DISCUSSION

The most important coefficient for estimating the transport of nanoparticles is the normalized effective diffusion coefficient

$$K_2 = \left(\frac{D_{eff}}{D_m} - \frac{A(\xi_c)^2 - 1}{A(\xi_c)^2} \right) \frac{A(\xi_c)^2}{Pe_0^2} \tag{35}$$

in that it gives a measure of the propensity of the particles to spread about their center of mass along the capillary. Differently from all the schemes proposed so far, the K_2 presented in **Eq.35** changes with ζ due to the variation of the mean fluid velocity along the permeable vessel. In **Figure 2** the relation $192(K_2 - Pe_c^{-2})$ was plotted as a function of ζ and τ in the case of large permeability of the walls ($\Pi = 8$, $\Omega = -2$) and for a Newtonian

fluid ($\xi_c = 0$). Generally K_2 increases with time and attains the steady state value after the early stage of dispersion which corresponds to $\tau = 0.5$. A central position of the vessel was observed where $K_2 - P_e^{-2} = 0$, implying that in such area dispersion is solely driven by pure molecular diffusion. The decrease of K_2 with ζ strongly depends upon the permeability of the capillary (Π) and the plug radius of the fluid (ξ_c). In **Figure 3** the 3D plot of the relation $192(K_2 - P_e^{-2})$ as a function of time τ and position along the capillary ζ was displayed showing the effects of Π and ξ_c varying between 0 and 4 and 0 and 0.4 respectively, and for a constant $\Omega = -2$. In **Figure 4**, the contourplots corresponding to **Figure 3** were reported. As time increases, the solution for K_2 tends to a constant asymptotic value. Noticeably, the time beyond which dispersion turns to be time independent is always less than 0.5, regardless Π and ξ_c . Therefore, the permeability parameter and the plug radius have a negligible effect upon the process of diffusion along with time but do effect on the steady state behavior of the system. In particular, when both Π and ξ_c are larger than zero the reduction in dispersion (D_{eff} or K_2) is dramatic, and in large portions of the capillary the transport of the nanoparticles is

mostly diffusion limited. This is easily explained observing that longitudinal transport is enhanced by radial velocity gradients (shear diffusion), thereby either an increase of the core region of the capillary with a flat velocity profile (thus ξ_c) or a reduction in the velocity amplitude due to an augmented permeability (thus Π), generates a decrease in K_2 , as thoroughly discussed in [8,9].

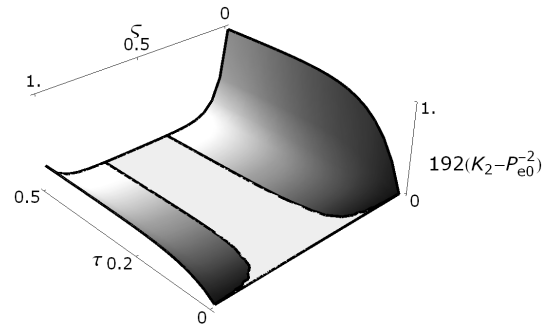


Figure 2. The dimensionless effective diffusion K_2 as a function of the normalized position (ζ) and time (τ) for a fixed plug radius $\xi_c = 0$ and for a permeable capillary ($\Pi = 8, \Omega = -2$).

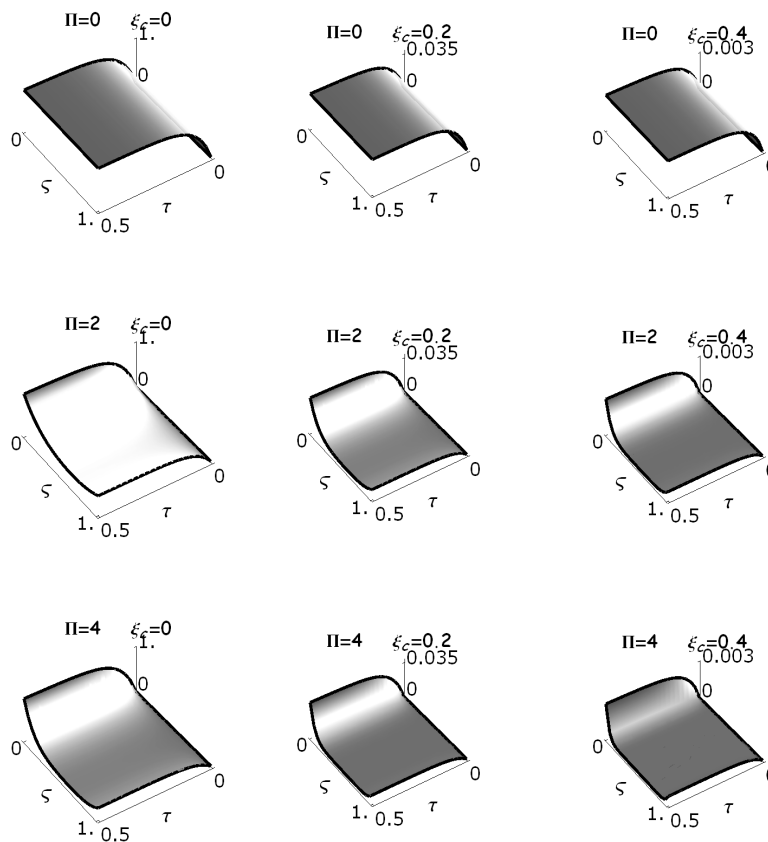


Figure 3. 3D plots of the dimensionless effective diffusion coefficients K_2 as a function of the normalized position (ζ) and time (τ), for Π and ξ_c varying between 0 and 4, and 0 and 0.4 respectively, and for a constant $\Omega = -2$.

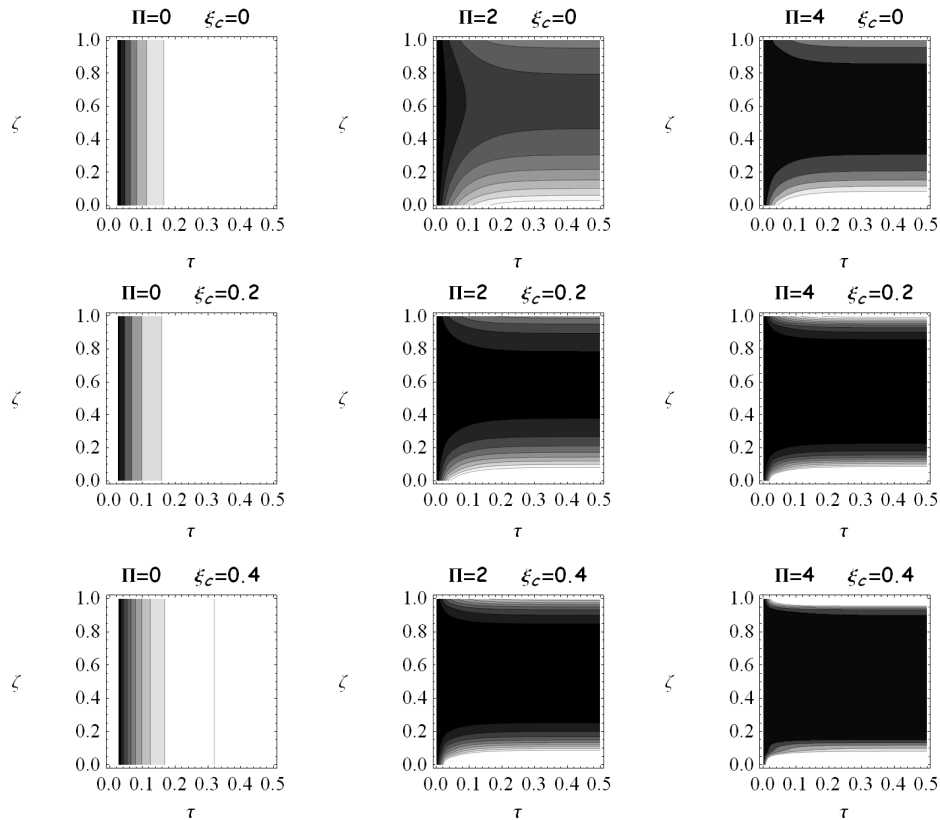


Figure 4. Contour plots of the dimensionless effective diffusion coefficients K_2 as a function of the normalized position (ζ) and time (τ), for Π and ξ_c varying between 0 and 4, and 0 and 0.4 respectively, and for a constant $\Omega = -2$.

Given K_2 , the effective diffusion coefficient D_{eff} was deduced as

$$D_{eff} = \frac{R_e^2 u_0^2}{A(\xi_c)^2 D_m} K_2 + \frac{A(\xi_c)^2 - 1}{A(\xi_c)^2} D_m, \tag{36}$$

or, equivalently

$$\frac{D_{eff}}{D_m} = \frac{P_{e_0}^2}{A(\xi_c)^2} K_2 + \frac{A(\xi_c)^2 - 1}{A(\xi_c)^2}. \tag{37}$$

Eq.37 shows that any enhancement in effective diffusion over the Brownian diffusion (D_m) is proportional to the product $P_{e_0} \times K_2$ and would strongly depend on the local hydrodynamics and capillary size.

The dimensionless effective diffusion D_{eff}/D_m as a function of the rheological parameter ξ_c , for different values of P_e and for a fixed $\Pi = 0$ was shown in **Figure 5**. As expected, confirming the results derived in [9], larger P_e and smaller ξ_c lead to larger D_{eff}/D_m ratios. **Figure 6** illustrated the ratio D_{eff}/D_m over time, for an impermeable channel ($\Pi = 0$) and for different values of ξ_c . **Figure 7** reported the same diagram of **Figure 6** for a permeable channel ($\Pi = 2$, $\Omega = -2$). In all cases, a steady state value was attained for τ larger than 0.5. Notice that for $\Pi = 0$ and for ξ_c moving

from 0 to 0.4, at large times the classical solutions of Taylor and Aris [1,2] ($\xi_c = 0$), and Sharp [4] ($\xi_c = 0.2, 0.4$) are recovered (**Figure 6**). When the permeable solution was instead considered (**Figure 7**), the steady state values recapitulated the results given by Decuzzi *et al.* [8] ($\xi_c = 0$) and Gentile *et al.* [9] ($\xi_c = 0.2, 0.4$).

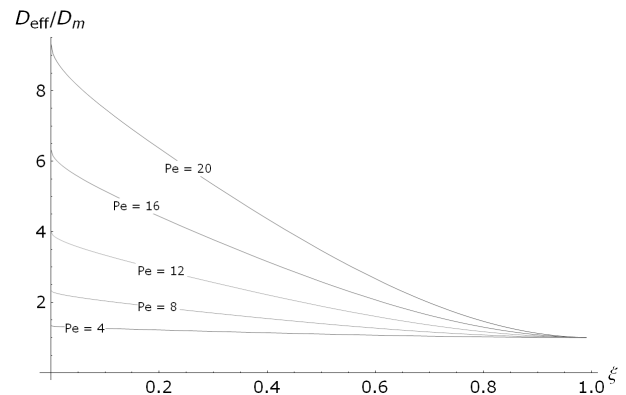


Figure 5. The dimensionless effective diffusion (D_{eff}/D_m) as a function of the rheological parameter ξ_c , for different values of P_e and for a fixed $\Pi = 0$.

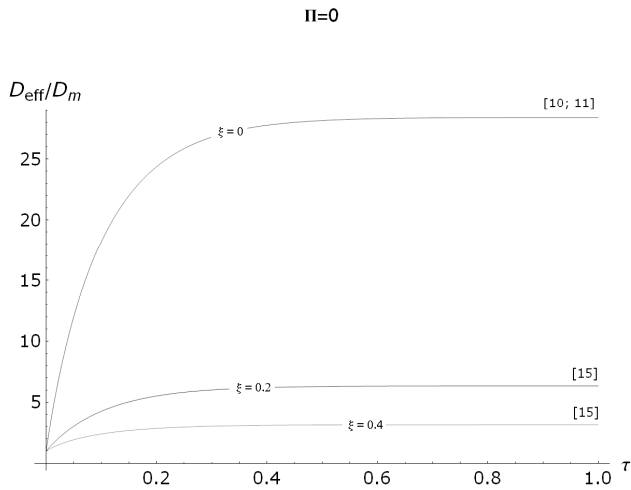


Figure 6. The ratio (D_{eff}/D_m) over time, for a permeable channel ($\Pi = 0$) and for different values of ξ_c .

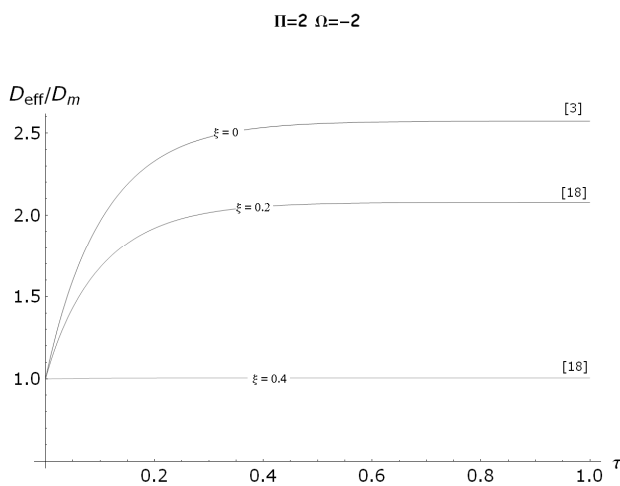


Figure 7. The ratio (D_{eff}/D_m) over time, for a permeable channel ($\Pi = 2$; $\Omega = -2$) and for different values of ξ_c .

Table 1. Average dimensions and velocities of blood vessels (Decuzzi, 2006 [8]). P_e is calculated for $D_m = 6 \times 10^{-13} \text{ m}^2/\text{s}$.

Vessel	L[mm]	R_c [mm]	U[mm/s]	P_e
Aorta	50	25	400	1.6×10^{10}
Artery	1.5-2	4	100	6.67×10^8
Arteriole	1.5-2	0.02-0.1	5	$1.67 - 8.33 \times 10^5$
Capillary	0.5	0.005-0.001	0.1-1	833-41667
Venules	1	0.02-0.05	0.5	$1.66 - 4.16 \times 10^4$
Vein	1-14	2-5	50	$1.6 - 4.1 \times 10^8$
Vena Cava	40-50	30	100	5×10^9

Recalling that the width of the plug radius ξ_c scales with R_e as $\xi_c \sim 1-3 \times R_e^{-0.8}$ [9] and considering the data of

Table 1, moving from capillaries to arterioles and venules P_{e_0} significantly increases and the ratio D_{eff}/D_m augments accordingly despite a reduction of the cell free layer area. **Figure 8** showed the minimum value that D_{eff}/D_m would assume in a vessel at the steady state as a function of Re and of the plug radius ξ_c for an impermeable vessel ($\Pi = 0$). **Figure 9** reported the same diagram for a permeable vessel ($\Pi = 5$, $\Omega = -2$). It was observed

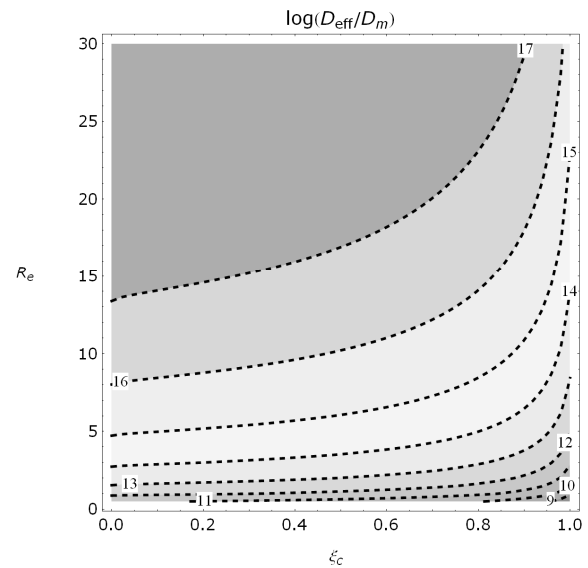


Figure 8. The minimum value that D_{eff}/D_m would assume in a vessel at the steady state as a function of Re and of the plug radius ξ_c ; for an impermeable vessel ($\Pi = 0$).

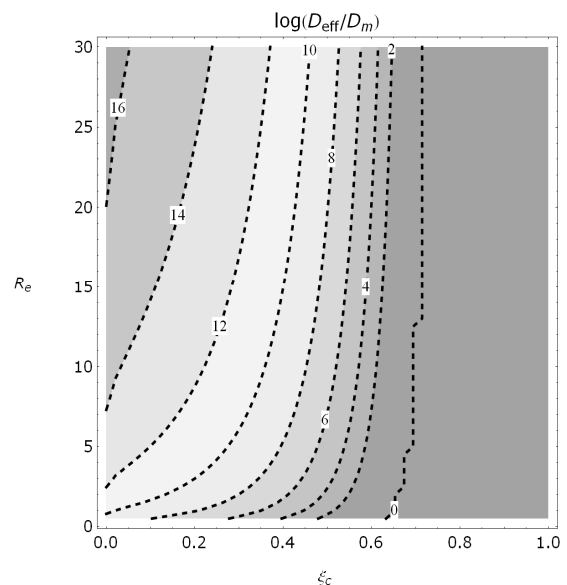


Figure 9. The minimum value that D_{eff}/D_m would assume in a vessel at the steady state as a function of Re and of the plug radius ξ_c ; for a permeable vessel ($\Pi = 5$, $\Omega = -2$).

that the effect of the radius of the vessel (or equivalently of P_{c0} , see **Table 1**) dominates over that of the plug radius, meaning that in large capillaries, where ξ_c is large, yet the longitudinal diffusion increases up to 10^6 times with respect to small vessels. And this effect is dramatically amplified considering leaky or fenestrated capillaries. It was argued in [8,9] that in a capillary network passively transported molecules or nanoparticles would follow the path with the largest effective diffusion. Therefore, nanoparticles and molecules would in a larger percentage stay in the macrocirculation (high D_{eff}) rather than in the microcirculation (small D_{eff}) or highly permeable vessels (even smaller D_{eff}), as for instance in the angiogenic tumor vasculature. This would constitute a barrier to the rational systemic administration of therapeutic and contrast agents. The correct design of nanoparticles could constitute an effective way to overcome this barrier. It was demonstrated, either experimentally [11-13] and theoretically [14], that particles having different sizes or shapes also have different margination properties, that is the attitude of “spontaneously” drifting towards the walls of the blood vessels. In particular, in considering the case of spherical particles, it was shown that the delivery efficiency is not size independent, instead larger particles would perform better than smaller ones under the effect of a gravitational or magnetic field [11]; whereas, below a characteristic diameter, the settling of nanoparticles would be mostly size independent [13]. In considering shapes other than spherical, it was demonstrated that, in the range of physiological relevant values of shear rates, inertial discoidal particles perform better than quasi-hemispherical and significantly better than spherical, and this circumstance would suggest the use of discoidal carriers in drug delivery [12,14].

In sight of the above findings, it is understandable that tailoring the shape and size of nanovectors inasmuch that they would tend to accumulate in the ‘cell free layer’, could significantly increase the efficiency of delivery.

4. CONCLUSIONS

The Generalized Dispersion Model firstly introduced by Gill and Sankarasubramanian was revised to account for blood rheology and vessel permeability. The non dimensional coefficient of diffusion was derived as a function of time, of the plug radius ξ_c and of a subset of permeability parameters, Π and Ω . It was observed that an enhancement in permeability or a blunted velocity profile (high hematocrit) dramatically reduces vascular transport. It was seen that an augmented permeability at the vessels walls does not influence the time in correspondence of which the dispersion process attains the

steady state. Evidence was given that freely administered drugs or nanoparticles very harshly would leave the macrocirculation in favour of leaky capillaries of tumor districts. Strategies for the avoidance of this physiological barrier were proposed.

REFERENCES

- [1] Taylor, G. (1953) Dispersion of soluble matter in solvent flowing slowly through a tube. *Proceedings of the Royal Society of London, A*, **219(1137)**, 186-203.
- [2] Aris, R. (1956) On the dispersion of a solute in a fluid flowing through a tube. *Proceedings of the Royal Society of London, A*, **235(1200)**, 67-77.
- [3] Gill, W.N. (1967) A note on the solution of transient dispersion problems. *Proceedings of the Royal Society of London, A*, **298(1967)**, 335-339.
- [4] Sankarasubramanian, R. and Gill, W.N. (1973) Taylor diffusion in laminar flow in an eccentric annulus. *Proceedings of the Royal Society of London, A*, **333**, 115-132.
- [5] Sharp, M.K. (1993) Shear-augmented dispersion in non-Newtonian fluids. *Annals of Biomedical Engineering*, **21(4)**, 407-415.
- [6] Dash, R.K., Jayaraman, G. and Mehta, K.N. (2000) Shear augmented dispersion of a solute in a cationic fluid flowing in a conduit. *Annals of Biomedical Engineering*, **28(4)**, 373-385.
- [7] Nagarani, P., Sarojamma, G. and Jayaraman, G. (2004) Effect of boundary absorption in dispersion in cationic fluid flow in a tube. *Annals of Biomedical Engineering*, **32(5)**, 706-719.
- [8] Decuzzi, P., Causa, F., Ferrari, M. and Netti, P.A. (2006) The effective dispersion of nanovectors within the tumor microvasculature. *Annals of Biomedical Engineering*, **34(4)**, 633-641.
- [9] Gentile, F., Ferrari, M. and Decuzzi, P. (2008) The transport of nanoparticles in blood vessels: The effect of vessel permeability and blood rheology. *Annals of Biomedical Engineering*, **2(36)**, 254-261.
- [10] Gill, W.N. and Sankarasubramanian, R. (1970) Exact analysis of unsteady convective diffusion. *Proceedings of the Royal Society of London, A*, **316**, 341-350.
- [11] Decuzzi, P., Gentile, F., Granaldi, A., Curcio, A. and Indolfi, C. (2007) Flow chamber analysis of size effects in the adhesion of spherical particles. *International Journal of NanoMedicine*, **2(4)**, 1-8.
- [12] Gentile, F., Chiappini, C., Fine, D., Bhavane, R.C., Pelucchio, M.S., Cheng, M., Liu, X., Ferrari, M. and Decuzzi, P. (2008) The margination dynamics of non spherical inertial particles in a microchannel. *Journal of Biomechanics*, **41(10)**, 2312-2318.
- [13] Gentile, F., Curcio, A., Indolfi, C., Decuzzi, P. and Ferrari, M. (2008) The margination propensity of spherical particles for vascular targeting in the microcirculation. *Journal of Nanobiotechnology*, **6(9)**, 1-9.
- [14] Lee, S.Y., Ferrari, M. and Decuzzi, P. (2009) Design of bio-mimetic particles with enhanced vascular interaction. *Journal of Biomechanics*, **42(12)**, 1885-1890.